

## ATR-SEIRAS Investigation of the Fermi Level of Pt Cocatalyst on a GaN Photocatalyst for Hydrogen Evolution under Irradiation

Masaaki Yoshida,<sup>†</sup> Akira Yamakata,<sup>‡</sup> Kazuhiro Takanabe,<sup>†</sup> Jun Kubota,<sup>†</sup> Masatoshi Osawa,<sup>‡</sup> and Kazunari Domen<sup>\*†</sup>

Department of Chemical System Engineering, The University of Tokyo, 7-3-1 Hongo, Bunkyo-ku, Tokyo 113-8656, Japan, and Catalysis Research Center, Hokkaido University, N-21 W-10, Kita-ku, Sapporo 001-0021, Japan

Received June 18, 2009; E-mail: domen@chemsys.t.u-tokyo.ac.jp

Photocatalytic overall water splitting is a promising technology for the sustainable production of hydrogen gas as an energy carrier.<sup>1,2</sup> Substantial efforts in recent years have led to the development of many photocatalysts for overall water splitting at ambient temperature under irradiation.<sup>1–4</sup> Modification with metal cocatalysts, essential components of the photocatalytic system, of photocatalysts greatly enhances their overall photocatalytic efficiency.<sup>2</sup> The interfacial electron transfer processes between a photocatalyst and a cocatalyst are yet to be investigated to understand the reaction mechanism and improve efficiency.

Kamat and co-workers observed a relative shift in the Fermi level equilibration of Au/TiO<sub>2</sub> nanocomposites by irradiation using a probe-redox couple of C<sub>60</sub>/C<sub>60</sub><sup>−</sup> in the solution.<sup>5</sup> In situ attenuated total reflection surface-enhanced infrared absorption spectroscopy (ATR-SEIRAS) is a powerful method to obtain vibrational information of surface molecules.<sup>6–8</sup> The frequency of adsorbed CO on a Pt electrode corresponds to the electrode potential.<sup>7,8</sup> Thus, the Fermi level of a Pt cocatalyst can be directly estimated from this ATR-SEIRAS measurement by following the CO vibrational frequency on the cocatalyst. Our group has recently demonstrated that a GaN photocatalyst powder has potential for overall water splitting under UV irradiation with a suitable cocatalyst.<sup>4</sup> We probed the Fermi level of a Pt cocatalyst in the working state on a GaN photocatalyst under UV irradiation by in situ ATR-SEIRAS measurements.

An epitaxially grown n-type GaN substrate (20 mm × 20 mm × 3 μm) on sapphire was used as a photocatalyst under the rest potential or as an electrode under potential control.<sup>9</sup> Pt particles were deposited on the GaN photocatalyst electrode as a cocatalyst for hydrogen evolution by electroless deposition and photodeposition.<sup>7</sup> Scanning electron microscopy (SEM) confirmed that the Pt cocatalysts were homogeneously deposited with particle sizes of 200–300 nm (Figure S1). Steady-state hydrogen evolution from aqueous MeOH was observed using the prepared samples (Figure S2), indicating that the prepared Pt/GaN sample was a reasonable model of a photocatalyst for hydrogen evolution.

The SEIRAS measurements of the GaN photocatalyst electrode were performed in CO-saturated aqueous solutions containing 0.1 M Na<sub>2</sub>SO<sub>4</sub> at various potentials under dark conditions or at rest potential under UV irradiation by high-pressure Hg lamp (see Figure S3).<sup>7</sup> Electrode potentials were measured against a Ag/AgCl reference electrode but are shown with respect to the standard hydrogen electrode (SHE). The cyclic voltammogram of the Pt/GaN photocatalyst electrode in CO saturated solution indicates that the adsorbed CO suppresses proton adsorption and the hydrogen evolution reaction on the electrode (See Figure S4).<sup>7a</sup> In addition,

from the potential point of view, the photogenerated holes can oxidize water (or CO) during these SEIRAS measurements and these oxidation reactions should predominantly occur on GaN rather than on Pt.<sup>9</sup> These results certify that shift of CO peaks during SEIRAS measurements under irradiation solely reflects the change in the potential caused by photoexcitation.

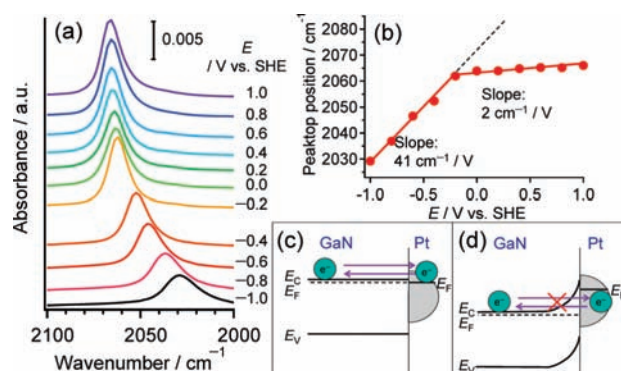


**Figure 1.** (a) Potential-dependent SEIRA spectra of adsorbed CO on Pt cocatalyst with potential control of the GaN photocatalyst electrode under dark conditions in CO-saturated aqueous solution of 0.1 M Na<sub>2</sub>SO<sub>4</sub>. Reference spectrum was measured under bubbling Ar prior to CO bubbling. (b) Plot of frequency vs potential for adsorbed CO on the Pt cocatalyst of the GaN photocatalyst electrode. Schematic model of electron transfer between the Pt cocatalyst and the GaN photocatalyst electrode under negative (c) and positive (d) potential control.

Figure 1a shows SEIRA spectra of adsorbed CO on the Pt cocatalyst at various potentials of the GaN photocatalyst electrode under dark conditions. The CO vibrational frequencies were observed at 2029–2066 cm<sup>−1</sup> between −1.0 and 1.0 V. The correlation between the CO peak frequencies and potentials is shown in Figure 1b. At potentials below −0.2 V, the voltage–frequency slope was 41 cm<sup>−1</sup>/V, which coincided with the reported value for a Pt electrode (~30 cm<sup>−1</sup>/V),<sup>7a</sup> suggesting that the frequencies of CO on the Pt cocatalyst correspond to the potentials of the GaN photocatalyst electrode (Figure 1c). At potentials above −0.2 V, the frequencies were nearly independent of the potentials of the GaN photocatalyst electrode (2 cm<sup>−1</sup>/V), indicating that electron migration between Pt and GaN was restricted, due to band bending derived from the n-type semiconductor, GaN (Figure 1d). Note that the inflection point of −0.2 V can be regarded as a flat band potential between the Pt cocatalyst and the GaN photocatalyst electrode, consistent with previous work,<sup>9</sup> although the value was not equivalent to the difference of work functions of GaN: 4.1 eV and Pt: 5.4 eV.<sup>10</sup>

The Fermi level of the Pt cocatalyst can be estimated by the measured CO frequencies and the potential–frequency plot with a

<sup>†</sup> The University of Tokyo.

<sup>‡</sup> Hokkaido University.

slope of  $41 \text{ cm}^{-1}/\text{V}$  in Figure 1b. Figure 2a,b shows irradiation time dependent SEIRA spectra of adsorbed CO on the Pt cocatalyst and Pt potentials estimated from the measured CO band, respectively. Before irradiation, a peak was observed at  $2066 \text{ cm}^{-1}$ , corresponding to a Pt cocatalyst potential of  $-0.09 \text{ V}$ . After irradiation for 1–5 s, the peak shifted to  $2073 \text{ cm}^{-1}$ , i.e.,  $0.08 \text{ V}$  for the Fermi level of the Pt cocatalyst. This positive shift indicates that hole immigrations were dominant compared with electron ones on some of the Pt particles at initial stage because of the upward band bending derived from the n-type GaN semiconductor being larger than a micrometer ( $\sim 3 \mu\text{m}$ ). Thereafter, the lower frequency peak at  $2056 \text{ cm}^{-1}$  appeared gradually, suggesting that the Fermi level of some of the Pt particles shifted to  $-0.35 \text{ V}$ , almost consistent with the hydrogen evolution potential ( $-0.50 \text{ V}$  under Ar; see Figure S4). This negative shift was due to the transfer of photogenerated electrons into the Pt cocatalyst as a result of charge separation, which is the essential function of cocatalysis for hydrogen evolution. It is interesting to note that, even after 90 s, the higher frequency peak remained at  $\sim 2074 \text{ cm}^{-1}$ , indicating that some Pt particles kept trapping the holes and possibly acted as recombination sites. After the lamp was turned off, the lower frequency peak gradually shifted to the initial position within ca. 15 min, while the higher frequency peak instantaneously disappeared. A similar result was obtained even in the solution including MeOH (see Figure S5), suggesting that the frequency shifts were not affected predominantly by surface oxidation reactions. At the lower light intensity ( $6.7 \times 10^{17} \text{ photon cm}^{-2} \text{ h}^{-1}$ ) no significant negative or positive shifts were observed (see Figure S6), indicating that the charge separation increases at higher light intensity.

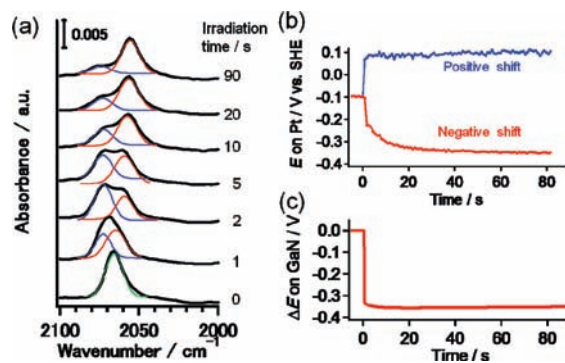


**Figure 2.** (a) Irradiation time dependent SEIRA spectra of adsorbed CO on Pt cocatalyst at the rest potential of the GaN photocatalyst electrode in CO saturated  $0.1 \text{ M Na}_2\text{SO}_4$  aqueous solution at light intensities of  $8.6 \times 10^{18} \text{ photon cm}^{-2} \text{ h}^{-1}$ . The curve-fitting results were shown in each spectrum using Gaussian functions. Reference spectrum was measured under bubbling Ar prior to CO bubbling. Time dependence of the estimated potential on the Pt cocatalyst with deconvolution processing (b) and the rest potential of the GaN photocatalyst electrode (c) during in situ ATR-SEIRAS measurement under irradiation.

The change in the rest potential of the GaN photocatalyst electrode under irradiation was also measured (Figure 2c). A negative shift of  $-0.35 \text{ V}$  was observed under irradiation at  $8.6 \times 10^{18} \text{ photon cm}^{-2} \text{ h}^{-1}$ , consistent with that of Pt cocatalyst measured by SEIRAS ( $\Delta E$ : ca.  $-0.25 \text{ V}$ ). The potential shift was observed within 1 s after irradiation although that of the Pt cocatalyst measured by SEIRAS gradually shifted until 20 s, indicating that the apparent electron transfer from GaN photocatalyst to Pt cocatalyst was considerably slow. It is reported that carrier injection at the Pt/TiO<sub>2</sub> interface is much faster (within  $1 \mu\text{s}$ ).<sup>11</sup> The slow

response of the potential shift may reflect the slow accumulation of electrons in Pt as a result of competitive electron and hole immigrations from GaN to Pt. This result suggests that the Fermi level of Pt cocatalyst is not consistently the same as that of the GaN photocatalyst. Thus, the information about the Fermi level of the Pt cocatalyst during the working state is important to develop more efficient photocatalysts.

This study demonstrates the first successful direct probing of the Fermi level of cocatalyst (Pt) on photocatalyst (GaN) during UV irradiation by in situ ATR-SEIRAS measurement with monitoring of the adsorbed CO vibrational frequency. This method can monitor the Fermi level shift by charge separation, which is the essential driving force for photocatalytic water splitting. It is also notable that the Fermi level of some Pt cocatalyst sites remained positive, as they possibly functioned as recombination sites for photogenerated electrons and holes. This probing method can be applied to many other photocatalyst systems to reveal the working state of charge separation during water splitting.

**Acknowledgment.** This work was supported by Tokyo Metropolitan CREATE, JST, and MEXT of Japan; Research and Development in a New Interdisciplinary Field Based on Nanotechnology and Materials Science program, Grant-in-Aid for Young Scientists (A) and Priority Areas 477 and 470, and the GCOE Program for Chemistry Innovation.

**Supporting Information Available:** Experimental procedures, characterizations of samples, schematic illustration of in situ SEIRAS, photocatalytic activity, electrochemical measurement, and SEIRA spectra in MeOH aq. solution or at different intensities. This material is available free-of-charge via the Internet <http://pubs.acs.org>.

## References

- (1) (a) Wang, X.; Maeda, K.; Thomas, A.; Takanabe, K.; Xin, G.; Carlsson, J. M.; Domen, K.; Antonietti, M. *Nat. Mater.* **2009**, *8*, 76–80. (b) Maeda, K.; Teramura, K.; Lu, D.; Takata, T.; Saito, N.; Inoue, Y.; Domen, K. *Nature* **2006**, *440*, 295.
- (2) (a) Kudo, A.; Miseki, Y. *Chem. Soc. Rev.* **2009**, *38*, 253–278. (b) Inoue, Y. *Energy Environ. Sci.* **2009**, *2*, 364–386. (c) Osterloh, F. E. *Chem. Mater.* **2008**, *20*, 35–54. (d) Maeda, K.; Domen, K. *J. Phys. Chem. C* **2007**, *111*, 7851–7861. (e) Hoertz, P. G.; Mallouk, T. E. *Inorg. Chem.* **2005**, *44*, 6828–6840. (f) Lee, J. S. *Catal. Surv. Asia* **2005**, *9*, 217–227.
- (3) (a) Maeda, K.; Takata, T.; Hara, M.; Saito, N.; Inoue, Y.; Kobayashi, H.; Domen, K. *J. Am. Chem. Soc.* **2005**, *127*, 8286–8287. (b) Maeda, K.; Teramura, K.; Lu, D.; Saito, N.; Inoue, Y.; Domen, K. *Angew. Chem., Int. Ed.* **2006**, *45*, 7806–7809. (c) Lee, Y.; Terashima, H.; Shimodaira, Y.; Teramura, K.; Hara, M.; Kobayashi, H.; Domen, K.; Yashima, M. *J. Phys. Chem. C* **2007**, *111*, 1042–1048. (d) Lee, Y.; Teramura, M.; Hara, M.; Domen, K. *Chem. Mater.* **2007**, *19*, 2120–2127.
- (4) Maeda, K.; Teramura, K.; Saito, N.; Inoue, Y.; Domen, K. *Bull. Chem. Soc. Jpn.* **2007**, *80*, 1004–1010.
- (5) (a) Subramanian, V.; Wolf, E. E.; Kamat, P. V. *J. Am. Chem. Soc.* **2004**, *126*, 4943–4950. (b) Jakob, M.; Levanon, H.; Kamat, P. V. *Nano Lett.* **2003**, *3*, 353–358. (c) Kamat, P. V. *Pure Appl. Chem.* **2002**, *74*, 1693–1706.
- (6) (a) Osawa, M. *Bull. Chem. Soc. Jpn.* **1997**, *70*, 2861–2880. (b) Uchida, T.; Mogami, H.; Yamakata, A.; Sasaki, Y.; Osawa, M. *J. Am. Chem. Soc.* **2008**, *130*, 10862–10863.
- (7) (a) Samjeské, G.; Komatsu, K.; Osawa, M. *J. Phys. Chem. C* **2009**, *113*, 10222–10228. (b) Yamakata, A.; Osawa, M. *J. Am. Chem. Soc.* **2009**, *131*, 6892–6893. (c) Yamakata, A.; Uchida, T.; Kubota, J.; Osawa, M. *J. Phys. Chem. B* **2006**, *110*, 6423–6427. (d) Miki, A.; Ye, S.; Osawa, M. *Chem. Commun.* **2002**, 1500–1501.
- (8) (a) Shiroishi, H.; Ayato, Y.; Kunimatsu, K.; Okada, T. *J. Electroanal. Chem.* **2005**, *581*, 132–138. (b) Kunimatsu, K.; Golden, W. G.; Seki, H.; Philpott, M. R. *Langmuir* **1985**, *1*, 245–250.
- (9) Ono, M.; Fujii, K.; Ito, T.; Iwaki, Y.; Hirako, A.; Yao, T.; Ohkawa, K. *J. Chem. Phys.* **2007**, *126*, 054708.
- (10) (a) Pankove, J. I.; Schade, H. *Appl. Phys. Lett.* **1974**, *25*, 53–55. (b) Surma, S. A. *Phys. Status Solidi* **2001**, *183*, 307–322.
- (11) Yamakata, A.; Ishibashi, T.; Osawa, M. *J. Phys. Chem. B* **2001**, *105*, 7258–7262.

JA904991P